

Article

Event-Triggered State Estimation for Uncertain Systems with Binary Encoding Transmission Scheme

Zun Li, Binqiang Xue * and Youyuan Chen

School of Automation, Qingdao University, Qingdao 266071, China

* Correspondence: xuebinqiang@qdu.edu.cn or xuebinqiang2005@163.com

Abstract: This paper proposes an event-triggered state estimation method for parameter-uncertain systems with a binary encoding transmission scheme. Firstly, a binary encoding transmission scheme is introduced between the state estimator and the system to improve the efficiency of network communication. Secondly, an event-triggering mechanism (ETM) is designed to ensure the accuracy of state estimation and reduce the computational burden of the state estimator. At the event-triggered moments, considering the uncertainty of the system, the binary encoding transmission scheme, and the ETM, a moving horizon estimator (MHER) is designed using the robust least squares optimization method to obtain optimal state estimation. At the no-event-triggered moments, the state estimation of the system is computed based on an open-loop state estimator (OLER). Furthermore, stability analysis showed that the state estimation error of the proposed method is bounded. Finally, the practical value of the proposed in this paper is confirmed through numerical simulation.

Keywords: moving horizon estimator (MHER); event-triggered mechanism (ETM); binary encoding transmission scheme; min–max problem

MSC: 93-10



Citation: Li, Z.; Xue, B.; Chen, Y. Event-Triggered State Estimation for Uncertain Systems with Binary Encoding Transmission Scheme. *Mathematics* **2023**, *11*, 3679. <https://doi.org/10.3390/math11173679>

Academic Editors: José Balthazar, Angelo Marcelo Tusset, Átila Madureira Bueno and Diego Colón

Received: 16 July 2023

Revised: 7 August 2023

Accepted: 10 August 2023

Published: 26 August 2023



Copyright: © 2023 by the authors. Licensee MDPI, Basel, Switzerland. This article is an open access article distributed under the terms and conditions of the Creative Commons Attribution (CC BY) license (<https://creativecommons.org/licenses/by/4.0/>).

1. Introduction

In recent years, state estimation theory has been extensively investigated [1–3]. Among the various state estimation methods, the moving horizon estimation (MHE) method continues to attract an increasing amount of attention because it can explicitly deal with constraints and limit the solutions of optimization problems to a fixed window length [4–6]. Using the moving horizon optimization principle, the authors of [7] designed a state estimation method with observable estimators for linear discrete systems. For distributed linear network systems, the authors of [8] proposed an MHE method with a consistent arrival cost. It is evident that the MHE method can provide solutions for state estimation problems in different systems.

Practical systems, such as robotic arms and unmanned aerial vehicles, are susceptible to external disturbances, which result in the uncertainty in the system model. However, state estimation for parameter-uncertain systems is challenging due to the uncertainty of the corresponding model parameters [9–11]. A regularized, robust method for dealing with uncertain data was proposed in [12], which effectively quantified the impact of uncertain parameters. The authors of [13] investigated the state estimation problem with respect to parameter-uncertain systems using min–max optimization theory. By designing a distributed moving horizon optimization algorithm for uncertain systems, the authors of [14] achieved good convergence of the state estimation error. The authors of [15] reduced the complexity of the state estimation scheme for distributed uncertain systems using a consistency algorithm.

At present, the time-triggered state estimation methods are mainly used for uncertain discrete systems, bringing about issues of limited communication bandwidth and energy shortages [16–20]. However, the event-triggered methods can effectively mitigate these

issues [21–23]. For linear systems with an energy-harvesting sensor, the authors of [24] designed a dynamic event-triggered state estimation method to compute the real-time estimation of system states. The authors of [25] introduced a state estimation algorithm for linear systems based on an ETM that ensured the smooth operation of a system when affected by issues such as insufficient communication bandwidth. To meet the requirements of high-intensity state estimation for complex systems, two event-triggered state estimation methods were proposed in [26] for centralized systems and distributed systems, respectively. In general, there is usually a considerable distance between the systems and the state estimators, so it is necessary to ensure the remote and efficient transmission of information [27–29]. The authors of [30] proposed a state estimation method with unknown inputs. It allowed for the accurate transmission of useful information by quantifying the system measurements. Ref. [31] presented a binary encoding scheme for centralized systems and distributed systems that was capable of effectively transmitting the output information of sensors. Furthermore, in practical systems, system noise and random measurement noise are usually energy-limited [32], and it is difficult to accurately compute their variances, means, and other properties. However, a distinctive feature in this regard is that the noise from a system and random measurements is usually bounded. Therefore, in order to further progress research in this area, it is important to predefine the upper bounds of system noise and random measurement noise [33,34].

In summary, uncertain systems in industrial production usually need to carry out remote information transmission in a timely manner. At the same time, the uncertain parameters lead to an obvious increase in the computational burden of state estimation, which can severely disrupt the normal functioning of systems. Therefore, it is crucial to propose a state estimation method for uncertain systems that not only achieves efficient and reliable information transmission but also enables accurate state estimation in cases involving limited computational resources.

Based on the above analysis, this paper proposes an event-triggered state estimation method for parameter-uncertain systems with a binary encoding transmission scheme. The main points of innovation are as follows:

- (1) By introducing a binary encoding transmission scheme, the efficient transmission of information between the state estimator and the system can be achieved.
- (2) By designing an ETM, the state is estimated via the OLER when an event is not triggered. When an event is triggered, the MHER developed in this study enables optimal state estimation by solving a min–max problem using a robust least squares optimization method.
- (3) Through stability analysis, the state estimation error is bounded when the noise remains bounded.

This paper consists of the following sections. Section 2 introduces the research subject and a flowchart of the designed state estimation method and presents the binary encoding transmission scheme and the ETM. In Section 3, the design process of the state estimator is described. The stability analysis is discussed in Section 4. Subsequently, Section 5 provides an example via a simulation. Finally, Section 6 provides a summary of the entire paper.

Given a symmetric positive definite matrix K , $\|\cdot\|_K^2$ is the square of the weighted Euclidean norm, $\|b\|_K^2 = b^T K b$. $\|\cdot\|$ represents the spectral norm of the matrix, and I represents the identity matrix. $E(\cdot)$ represents the expectation of the vector parameters, and \mathbf{R}^n stands for n -dimensional space. For the positive definite matrix K , $\lambda_{\max}(K)$ represents the maximum singular value of matrix K , and $\lambda_{\min}(K)$ represents the minimum singular value of matrix K . $\text{col}\{b_{t-N}, \dots, b_t\}$ is denoted as b_{t-N}^t .

2. Problem Description

2.1. System Model

Consider the following class of parameter-uncertain linear discrete systems:

$$\begin{aligned} x_{t+1} &= (A + \delta A_t)x_t + \omega_t, \\ y_t &= Cx_t + v_t, \end{aligned} \tag{1}$$

where $t \in \mathbf{N}_{\geq 0}$, $x_t \in \mathbf{X} \in \mathbf{R}^{n_x}$ represents the system state variable, $y_t \in \mathbf{Y} \in \mathbf{R}^{n_y}$ represents the measurement output, $\omega_t \in \mathbf{W} \subset \mathbf{R}^{n_x}$ denotes system noise, and $v_t \in \mathbf{V} \subset \mathbf{R}^{n_y}$ represents random measurement noise. A and C represent the matrices with appropriate dimensions. Additionally, the uncertainty of the model parameter is represented by δA_t , which is a matrix of the same type as A .

Assumption 1. The matrix group (C, A) is observable in N steps.

Assumption 2. Set \mathbf{X} , \mathbf{W} , and \mathbf{V} such that they satisfy the following conditions:

$$\begin{cases} \mathbf{X} = \{x_t : \|x_t\| \leq \rho_x\}, \\ \mathbf{W} = \{\omega_t : \|\omega_t\| \leq \rho_\omega\}, \\ \mathbf{V} = \{v_t : \|v_t\| \leq \rho_v\}, \end{cases}$$

where ρ_x , ρ_ω , and ρ_v represent the upper bounds of the state variable, system noise, and random measurement noise, respectively.

To cope with the complex network communication environment and ensure the efficient transmission of information, this paper introduces a binary encoding transmission scheme operating between the sensor and the state estimator. To reduce the estimation burden of the state estimator and ensure estimation accuracy, the ETM was designed. The state estimation method proposed in this paper is illustrated in Figure 1.

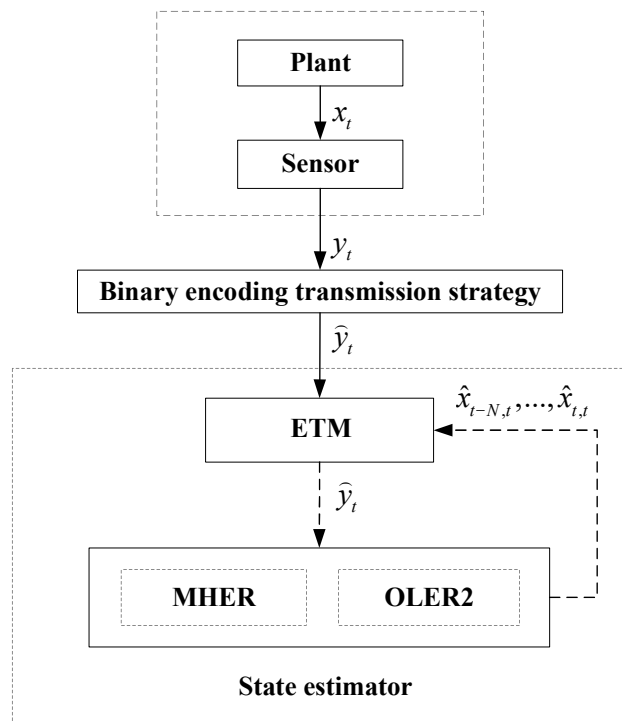


Figure 1. Event-triggered state estimation method.

2.2. Design of Binary Encoding Transmission Scheme

As shown in Figure 2, we designed a binary encoding transmission scheme for transmitting a sensor’s measurement output to a state estimator.



Figure 2. Binary encoding transmission scheme.

In the binary encoding transmission scheme, a constant scalar M_t within a certain range $[-U, U]$ is converted into a binary array with a length of Ω at time t . Then, 2^Ω points are obtained from the binary array, and $\chi = \{l_1, \dots, l_{2^\Omega}\}$ are used to represent these evenly spaced points. There are a total of $2^\Omega - 1$ equally long intervals, each with a length of $\zeta_l = 2U/2^\Omega - 1$. By utilizing a random truncation function, M_t is processed to obtain the truncated output β_t .

When $l_i \leq M_t \leq l_{i+1}$, $i = 1, 2, \dots, 2^\Omega - 1$, β_t is generated via the following equation:

$$\begin{cases} \mathbf{P}\{\beta_t(M_t, \Omega) = l_i\} = 1 - p_t, \\ \mathbf{P}\{\beta_t(M_t, \Omega) = l_{i+1}\} = p_t, \end{cases} \tag{2}$$

where $0 \leq p_t \leq 1$, $p_t = (M_t - l_i)/\zeta_l$. In addition, β_t can be obtained based on

$$\beta_t(M_t, \Omega) = -U + \sum_{i=1}^{\Omega} o_{i,t} 2^{i-1} \zeta_l. \tag{3}$$

Therefore, M_t is encoded into a binary array: $O_t = \{o_{1,t}, o_{2,t}, \dots, o_{\Omega,t}\}$, $o_{i,t} \in \{0, 1\}$.

To fulfill the requirement for transmitting the sensor measurement output, the designed encoding scheme is expanded into vector form: $M_t \in \mathbf{R}^{n_y}$, $\beta_t(M_t, \Omega) \in \mathbf{R}^{n_y}$.

To quantify the measurement output distortion caused by the binary encoding transmission scheme, the sensor measurement output recovered by the binary decoder is processed as follows:

$$\hat{y}_i = \beta_t(y_i, \Omega), i = t - N, \dots, t, \tag{4}$$

where $E\{\hat{y}_i\} = y_i$, N represents the window length of state estimation, and the truncation error is denoted as $\varepsilon_i = \hat{y}_i - y_i$. \mathfrak{S} represents the tight set that constrains the truncation error

$$\mathfrak{S} = \{\varepsilon_i \in \mathbf{R}^{n_y}, \|\varepsilon_{t-N}^t\| = \|\hat{y}_{t-N}^t - y_{t-N}^t\| \leq \omega, \omega > 0\}. \tag{5}$$

Remark 1. Different from the communication scheme designed in [31], the scheme designed in this paper only considers the error caused by the random truncation function in the communication process and restricts the truncation error. In actual information transmission, the probability of binary bit flipping in the binary coding transmission scheme is very low, and its error is negligible compared with the truncation error, so this problem is not studied in this paper.

2.3. Design of ETM

The ETM is set on the estimator’s side, and its configuration is illustrated in Figure 3.

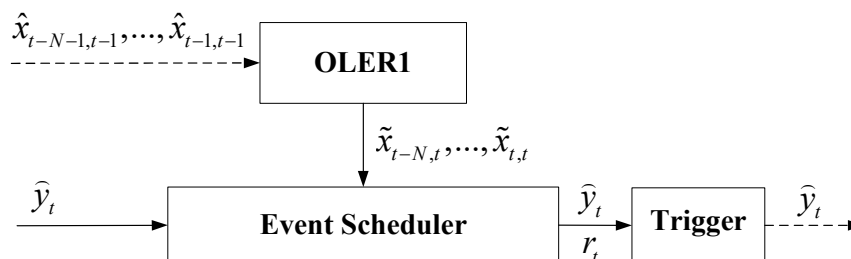


Figure 3. Schematic diagram of the ETM.

At $t > N$, the ETM obtains the output value after its transmission via the binary encoding transmission scheme, and OLER1 provides the current state estimation value; then,

the two values are both transmitted to the event scheduler, which performs a calculation based on the following conditions:

$$r_t = \begin{cases} 0, & \text{if } \left\| \hat{y}_{t-N}^t - \tilde{y}_{t-N,t}^{t,t} \right\| \leq \Delta, \\ 1, & \text{if } \left\| \hat{y}_{t-N}^t - \tilde{y}_{t-N,t}^{t,t} \right\| > \Delta, \end{cases} \tag{6}$$

where Δ is the threshold to adjust the event trigger; $r_t = 1$ and $r_t = 0$ respectively indicate whether the event has been triggered; $\tilde{y}_{i,t}$ satisfies

$$\tilde{y}_{i,t} = C\tilde{x}_{i,t}, i = t - N + 1, \dots, t, \tag{7}$$

$\tilde{x}_{i,t}$ represents the state estimation carried out by OLER1.

Based on the above analysis, at time t , the available information \bar{y}_t of the state estimator is satisfied:

$$\begin{cases} \bar{y}_t = \hat{y}_t, & \text{if } r_t = 1, \\ \bar{y}_t = \tilde{y}_{t,t}, & \text{otherwise.} \end{cases} \tag{8}$$

Then, the following equation is obtained

$$\left\| \hat{y}_{t-N}^t - \bar{y}_{t-N}^t \right\| \leq \left\| \hat{y}_{t-N}^t - \tilde{y}_{t-N,t}^{t,t} \right\| \leq \Delta. \tag{9}$$

To quantify the error caused by the ETM, we introduce a bounded vector g_i , $i = t - N, \dots, t$, which satisfies the following relation:

$$\|g_{t-N}^t\| = \left\| \hat{y}_{t-N}^t - \bar{y}_{t-N}^t \right\| \leq \left\| \hat{y}_{t-N}^t - \tilde{y}_{t-N,t}^{t,t} \right\| \leq \Delta. \tag{10}$$

Thus, the relationship between the available information \bar{y}_t regarding the state estimator and the system state variable x_t can be expressed as follows:

$$\bar{y}_t = Cx_t + v_t + \varepsilon_t + g_t. \tag{11}$$

3. Design of State Estimator

The state estimator is composed of OLER2 and an MHER. When $r_t = 1$, an MHER is stimulated to obtain the optimal state estimation sequences within the current time window. When $r_t = 0$, OLER2 is used to obtain the open-loop state estimation sequences within the current time window.

3.1. Design of OLER

$\tilde{x}_{i,t}$ represents the estimate of $x_{i,t}$. At $t > N$, the updated estimation sequences of state by the OLER1 are as follows:

$$\tilde{x}_{i+1,t} = A\tilde{x}_{i,t}, i = t - N, \dots, t, \tag{12}$$

$$\tilde{x}_{t-N,t} = A\tilde{x}_{t-N-1,t-1}, \tag{13}$$

$$\tilde{x}_{t-N-1,t-1} = \begin{cases} \hat{x}_{t-N-1,t-1}^*, & \text{if } r_{t-1} = 1, \\ \tilde{x}_{t-N-1,t-1}, & \text{if } r_{t-1} = 0. \end{cases} \tag{14}$$

The OLER2 designed in the state estimator has the same structure as OLER1.

Remark 2. OLER1 is designed to ensure that the ETM can operate properly when $t > N$. OLER2 is used to obtain the open-loop estimation of a state when an event has not been triggered, thus ensuring that the MHER can use the information from a previous moment when an event is triggered.

3.2. Design of MHER

At $t > N$, based on the MHE method, the cost function is as follows:

$$J = \|\hat{x}_{t-N,t} - \bar{x}_{t-N}\|_G^2 + \sum_{i=t-N}^t \|y_i - C\hat{x}_{i,t}\|^2, \tag{15}$$

where $y_i = \bar{y}_i - \varepsilon_i - g_i$, and G is the weighted positive-definite matrix. A vector $m_i = g_i + \varepsilon_i$ is introduced to represent the difference between the measurement output of the sensor and the available information on the state estimator, which satisfies the following relation:

$$\Psi = \{m_i \in \mathbf{R}^{n_y}, \|m_{t-N}^t\| = \|\varepsilon_{t-N}^t + g_{t-N}^t\| \leq \|\varepsilon_{t-N}^t\| + \|g_{t-N}^t\| \leq \varphi, \varphi > 0\}, \tag{16}$$

Therefore, Equation (8) can be written as

$$J = \|\hat{x}_{t-N,t} - \bar{x}_{t-N}\|_G^2 + \sum_{i=t-N}^t \|\bar{y}_i - C\hat{x}_{i,t} - m_i\|^2. \tag{17}$$

To account for the effect of the uncertain parameters $\delta A_i, i = t - N, \dots, t - 1$ and the output mismatch caused by m_i , this paper utilizes the robust least squares optimization method mentioned in [12,14]. Then, the following problems are introduced.

Problem 1. \bar{x}_{t-N} and \bar{y}_{t-N}^t are known, and the optimal estimate of the state $\hat{x}_{t-N,t}^*$ satisfies

$$\hat{x}_{t-N,t}^* = \arg \min_{\hat{x}_{t-N,t}} \max_{m_i, \delta A_i} J(\hat{x}_{t-N,t}, m_i, \delta A_i), i = t - N, \dots, t, \tag{18}$$

where $\hat{x}_{i,t}^* = A\hat{x}_{i-1,t}^*$; the prior estimate of state x_{t-N} is represented as

$$\bar{x}_{t-N} = \begin{cases} A\hat{x}_{t-N-1,t-1}^*, & \text{if } r_{t-1} = 1, \\ A\bar{x}_{t-N-1,t-1}, & \text{if } r_{t-1} = 0, \end{cases} \tag{19}$$

where $t > N$; and \bar{x}_0 represents the initial estimate of x_0 .

To facilitate the subsequent computations, define the following terms in the corresponding manner:

$$Q = \begin{bmatrix} C \\ CA \\ \vdots \\ CA^N \end{bmatrix}, \hat{Q}_t = \begin{bmatrix} C \\ C(A + \delta A_{t-N}) \\ \vdots \\ C \prod_{i=1}^N (A + \delta A_{t-i}) \end{bmatrix},$$

$$\Theta_t = \begin{bmatrix} 0 & \cdots & 0 & 0 \\ C & \cdots & 0 & 0 \\ \vdots & \vdots & \vdots & \vdots \\ C \prod_{i=1}^{N-1} (A + \delta A_{t-i}) & \cdots & C(A + \delta A_{t-i}) & C \end{bmatrix}.$$

Therefore, we can obtain the following:

$$\hat{x}_{t-N,t}^* = \arg \min_{\hat{x}_{t-N,t}} \max_{m_{t-N}^t, \delta A_{t-N}, \dots, \delta A_t} \left[\|\hat{x}_{t-N,t} - \bar{x}_{t-N}\|_G^2 + \|\bar{y}_{t-N}^t - \hat{Q}_t \hat{x}_{t-N,t} - m_{t-N}^t\| \right]. \tag{20}$$

By utilizing Equation (20) and Theorem 3.3 from [12], Problem 2 can be obtained.

Problem 2. \bar{x}_{t-N} and \bar{y}_{t-N}^t are known. The optimal estimate of state $\hat{x}_{t-N,t}^*$ satisfies

$$\hat{x}_{t-N,t}^* = \arg \min_{\hat{x}_{t-N,t}} \max_{\|f_t\| \leq \eta_1 \|\hat{x}_{t-N,t} - \bar{x}_{t-N,t}\| + \eta_2} \tilde{J}(\hat{x}_{t-N,t}, f_t), \tag{21}$$

where

$$\tilde{J}(\hat{x}_{t-N,t}, f_t) = \|\hat{x}_{t-N,t} - \bar{x}_{t-N}\|_G^2 + \left\| (Q + \tilde{Q}_t)(\hat{x}_{t-N,t} - \bar{x}_{t-N}) - (\bar{y}_{t-N}^t - Q\bar{x}_{t-N} - (\tilde{Q}_t\bar{x}_{t-N} + m_{t-N}^t)) \right\|^2, \tag{22}$$

$$\hat{x}_{i+1,t}^* = A\hat{x}_{i,t}^*, i = t - N, \dots, t - 1, \tag{23}$$

where $\tilde{Q}_t = \hat{Q}_t - Q$, $\|\tilde{Q}_t\| \leq \eta_1$, $\|\tilde{Q}_t\bar{x}_{t-N} + m_{t-N}^t\| \leq \eta_2$ and $\|f_t\| \leq \eta_1 \|\hat{x}_{t-N,t} - \bar{x}_{t-N}\| + \eta_2$, while η_1 and η_2 are two scalar parameters.

Regarding Problem 2, considering the case where $\hat{x}_{t-N,t}^* \neq 0$ and introducing a scalar parameter θ_t , ($\theta_t > 1$), we can obtain the following expression:

$$\hat{x}_{t-N,t}^* = \left(\hat{G}_t + (\theta_t^*/\theta_t^* - 1)Q^TQ \right)^{-1} \left((\theta_t^*/\theta_t^* - 1)Q^T\bar{y}_{t-N}^t + \hat{G}_t\bar{x}_{t-N} \right), \tag{24}$$

where θ_t^* represents the solution that minimizes θ_t , whose expression is as follows:

$$\theta_t^* = \arg \min_{\theta_t > 1} \Lambda(\theta_t). \tag{25}$$

The expression of $\Lambda(\theta_t)$ is as follows:

$$\Lambda(\theta_t) = \left\| (\hat{x}_{t-N,t} - \bar{x}_{t-N,t})^*(\theta_t) \right\|_G^2 + \theta_t S^2 \left((\hat{x}_{t-N,t} - \bar{x}_{t-N,t})^*(\theta_t) \right) + \left\| Q(\hat{x}_{t-N,t} - \bar{x}_{t-N,t})^*(\theta_t) - (\bar{y}_{t-N}^t - Q\bar{x}_{t-N}) \right\|_{(\theta_t/\theta_t-1)I}^2, \tag{26}$$

where $S(\hat{x}_{t-N,t} - \bar{x}_{t-N,t}) = \eta_1 \|\hat{x}_{t-N,t} - \bar{x}_{t-N,t}\| + \eta_2$.

In Equation (24), \hat{G}_t satisfies $\hat{G}_t = G + \theta_t^* \eta_1 (\eta_1 + \eta_2/\alpha_t^*(\theta_t^*))I$; here, $\alpha_t^*(\theta_t)$ is the unique solution of the following equation:

$$\alpha_t^2 = \left((\theta_t/\theta_t - 1)Q^T(\bar{y}_{t-N}^t - Q\bar{x}_{t-N}) \right)^T \left[G + (\theta_t/\theta_t - 1)Q^TQ + \theta_t \eta_1 (\eta_1 + \eta_2/\alpha_t)I \right]^{-2} \left((\theta_t/\theta_t - 1)Q^T(\bar{y}_{t-N}^t - Q\bar{x}_{t-N}) \right), \tag{27}$$

where $\alpha_t = \|\hat{x}_{t-N,t} - \bar{x}_{t-N,t}\|$.

Remark 3. Equation (24) is obtained by solving a min–max problem using the regularized robust least squares optimization method with bounded uncertainties. The specific solution process is detailed in [12].

Remark 4. As shown in Algorithm 1, the ETM only works when the time exceeds the length of the state estimation window N , and the MHER is always used for state estimation when the time is not exceeded. Unlike the methods in [25,26], this paper designs the ETM after remote network transmission has occurred, so the step involving the transmission of the estimated results to the plant side is omitted. The efficiency of state estimation is further improved.

Algorithm 1: The state estimation algorithm designed in this paper.

Step 1: At $t \leq N$, execute the following steps:

Step 1.1: Based on binary encoding transmission scheme, y_t is transmitted to obtain \hat{y}_t .

Step 1.2: Based on the design of the MHER, $\hat{x}_{0,t}^*, \dots, \hat{x}_{t,t}^*$ is obtained.

Step 2: At $t > N$, execute the following steps:

Step 2.1: Based on binary encoding transmission scheme, y_t is transmitted to obtain \hat{y}_t .

Step 2.2: Based on Equations (12)–(14), OLER1 calculates the value of $\tilde{x}_{t-N,t}, \dots, \tilde{x}_{t,t}$.

Step 2.3: Based on Equation (6), the event scheduler calculates the value of r_t .

If $r_t = 1$, based on Equations (21)–(24), the MHER obtains $\hat{x}_{0,t}^*, \dots, \hat{x}_{t,t}^*$.

If $r_t = 0$, based on Equations (12)–(14), OLER2 obtains $\tilde{x}_{t-N,t}, \dots, \tilde{x}_{t,t}$.

Step 3: To update \tilde{y}_{t-N}^t , let $t = t + 1$ and proceed to step 1.

4. Stability Analysis

The purpose of this section is to analyze whether the error of the designed event-triggered state estimation method is bounded under different event-triggered situations.

Referring to the relevant knowledge of linear matrix inequalities in [14], define the following as represented:

$$\begin{cases} \gamma_{\delta a} = \max_{\delta A_i, i=t-N, \dots, t-1} \|\delta A_i\|, \\ \gamma_{\tilde{Q}} = \max_{\delta A_i, i=t-N, \dots, t-1} \|\tilde{Q}_t\|, \\ \gamma_{\Theta} = \max_{\delta A_i, i=t-N, \dots, t-1} \|\Theta_t\|. \end{cases} \quad (28)$$

Based on the needs of stability analysis [35–37], define the following terms as they are shown:

$$\begin{cases} \sigma = \lambda_{\min}(\hat{G}_t), \\ \bar{\sigma} = \lambda_{\max}(\hat{G}_t), \\ q = \lambda_{\min}(Q^T Q), \\ \gamma_a = \|A\|, \\ \gamma_Q = \|Q\|. \end{cases} \quad (29)$$

Theorem 1 is introduced to analyze whether the state estimation error is bounded when OLER2 is used.

Theorem 1. Under the conditions that Assumptions 1 and 2 are satisfied, if $r_t = 0$, the open-loop estimated value $\tilde{x}_{t-N,t}$ of the state satisfies

$$\|x_{t-N} - \tilde{x}_{t-N,t}\| \leq Y, \quad (30)$$

where $Y = 1 / \sqrt{q}(\varphi + \gamma_{\Theta}\sqrt{N}\rho_{\omega} + \sqrt{N+1}\rho_v + \gamma_{\tilde{Q}}\rho_x)$.

Proof of Theorem 1. Based on Equations (1) and (7), we can determine that

$$y_{t-N}^t - \tilde{y}_{t-N}^t = (Q + \tilde{Q}_t)x_{t-N} + \Theta_t \omega_{t-N}^{t-1} + v_{t-N}^t - Q\tilde{x}_{t-N,t}, \quad (31)$$

Then, we can obtain the following:

$$Q(x_{t-N} - \tilde{x}_{t-N,t}) = (y_{t-N}^t - \tilde{y}_{t-N}^t) - (\Theta_t \omega_{t-N}^{t-1} + v_{t-N}^t + \tilde{Q}_t x_{t-N}). \quad (32)$$

If Assumptions 1 and 2 are satisfied, then $q > 0$ holds; thus, it can be concluded that

$$\begin{aligned} \|x_{t-N} - \bar{x}_{t-N,t}\| &\leq \frac{1}{\sqrt{q}} \left(\|y_{t-N}^t - \tilde{y}_{t-N}^t\| + \|\Theta_t\| \|\omega_{t-N}^{t-1}\| \right. \\ &\quad \left. + \|v_{t-N}^t\| + \|\tilde{Q}_t\| \|x_{t-N}\| \right) \\ &\leq \frac{1}{\sqrt{q}} \left(\varphi + \gamma_{\Theta} \sqrt{N} \rho_{\omega} + \sqrt{N+1} \rho_v + \gamma_{\tilde{Q}} \rho_x \right) \\ &= Y < +\infty. \end{aligned} \tag{33}$$

Thus, the proof of Theorem 1 is complete. \square

Theorem 1 proves that the state estimation error of the system is bounded when an event is not triggered. To analyze whether the state estimation error of system is bounded when an event is triggered, Theorem 2 is introduced.

Theorem 2. Under the conditions that Assumptions 1 and 2 are satisfied, if $r_t = 1$, the optimal estimate of the state obtained via the MHER satisfies

$$\|x_{t-N} - \hat{x}_{t-N,t}^*\| < Y_{t-N}, \tag{34}$$

where Y_{t-N} is defined below.

Proof of Theorem 2. Define $\hat{e}_{t-N,t} = x_{t-N} - \hat{x}_{t-N,t}^*$ and $\Xi(h) = \hat{G}_t(h) + (h/(h-1))Q^T Q$, $h > 1$. From Equation (11), we are left with

$$\tilde{y}_{t-N}^t = \hat{Q}x_{t-N} + \Theta\omega_{t-N}^{t-1} + v_{t-N}^t + m_{t-N}^t. \tag{35}$$

Based on Equations (24) and (35), $\hat{e}_{t-N,t}$ is expressed as follows:

$$\begin{aligned} \hat{e}_{t-N,t} &= \Xi(\theta_t^*)^{-1} [\hat{G}_t(x_{t-N} - \bar{x}_{t-N}) - (\theta_t^*/\theta_t^* - 1)Q^T \\ &\quad (\tilde{Q}x_{t-N} + \Theta\omega_{t-N}^{t-1} + v_{t-N}^t + m_{t-N}^t)]. \end{aligned} \tag{36}$$

At $t > N$, it can be derived from Equation (19) that

$$x_{t-N} - \bar{x}_{t-N} = \begin{cases} (A + \delta A_{t-N-1})x_{t-N-1} - A\hat{x}_{t-N-1,t-1}^* + \omega_{t-N-1}, & \text{if } r_{t-1} = 1, \\ (A + \delta A_{t-N-1})x_{t-N-1} - A\bar{x}_{t-N-1,t-1} + \omega_{t-N-1}, & \text{if } r_{t-1} = 0. \end{cases} \tag{37}$$

Additionally, the state estimation error satisfies

$$e_{t-N-1,t-1} = \begin{cases} x_{t-N-1} - \hat{x}_{t-N-1,t-1}^*, & \text{if } r_{t-1} = 1, \\ x_{t-N-1} - \bar{x}_{t-N-1,t-1}, & \text{if } r_{t-1} = 0. \end{cases} \tag{38}$$

By utilizing Equations (36)–(38), we can obtain the following:

$$\begin{aligned} \|\hat{e}_{t-N,t}\| &\leq \left\| \Xi(\theta_t^*)^{-1} \right\| \|\hat{G}_t\| \|A\| \|e_{t-N-1,t-1}\| + \left\| \Xi(\theta_t^*)^{-1} \right\| \|\hat{G}_t\| \|\delta A_{t-N-1}\| \|x_{t-N-1}\| \\ &\quad + \left\| \Xi(\theta_t^*)^{-1} \right\| \|\hat{G}_t\| \|\omega_{t-N-1}\| + \Pi(\theta_t^*) \|Q^T\| \|\tilde{Q}_t\| \|x_{t-N}\| \\ &\quad + \Pi(\theta_t^*) \|Q^T\| \|\Theta_t\| \|\omega_{t-N}^{t-1}\| + \Pi(\theta_t^*) \|Q\| \|v_{t-N}^t\| \\ &\quad + \Pi(\theta_t^*) \|Q\| \|m_{t-N}^t\|, \end{aligned} \tag{39}$$

where $\Pi(\theta_t^*) = (\theta_t^*/\theta_t^* - 1) \left\| \Xi(\theta_t^*)^{-1} \right\|$.

When $h > 1$, $\|\Xi(h)^{-1}\| = (1/\lambda_{\min}(\Xi(h)))$ is satisfied, and $\lambda_{\min}(\hat{G}_t) + (h/h - 1)\lambda_{\min}(Q^T Q) \leq \lambda_{\min}(\Xi(h))$ is also satisfied. Then, for $\theta_t^* > 1$, we can determine that

$$\|\Xi(\theta_t^*)^{-1}\|\|\hat{G}_t\| \leq \left(\lambda_{\min}(\hat{G}_t) + \left(\frac{\theta_t^*}{\theta_t^* - 1}\right)\lambda_{\min}(Q^T Q)\right)^{-1} \lambda_{\max}(\hat{G}_t). \tag{40}$$

If Assumptions 1 and 2 are satisfied, based on $\lambda_{\min}(Q^T Q) > 0$ and Equations (28), (29), and (40), we can conclude that

$$\|\Xi(\theta_t^*)^{-1}\|\|\hat{G}_t\|\|A\| < \frac{\lambda_{\max}(\hat{G}_t)\|A\|}{(\lambda_{\min}(\hat{G}_t) + \lambda_{\min}(Q^T Q))} = \frac{\bar{\sigma}\gamma_a}{\underline{\sigma} + \underline{q}}, \tag{41}$$

$$\|\Xi(\theta_t^*)^{-1}\|\|\hat{G}_t\|\|\delta A_{t-N-1}\|\|x_{t-N-1}\| < \frac{\lambda_{\max}(\hat{G}_t)\|\delta A_{t-N-1}\|\|x_{t-N-1}\|}{(\lambda_{\min}(\hat{G}_t) + \lambda_{\min}(Q^T Q))} = \frac{\bar{\sigma}\gamma_{\delta a}\rho_x}{\underline{\sigma} + \underline{q}}, \tag{42}$$

$$\|\Xi(\theta_t^*)^{-1}\|\|\hat{G}_t\|\|\omega_{t-N-1}\| < \frac{\lambda_{\max}(\hat{G}_t)\rho_{\omega}}{(\lambda_{\min}(\hat{G}_t) + \lambda_{\min}(Q^T Q))} = \frac{\bar{\sigma}\rho_{\omega}}{\underline{\sigma} + \underline{q}}. \tag{43}$$

The remaining terms in Equation (39) are processed as follows:

$$\begin{aligned} \Pi(\theta_t^*) &= \left(\frac{\theta_t^*}{\theta_t^* - 1}\right)\|\Xi(\theta_t^*)^{-1}\| \leq \left(\frac{\theta_t^*}{\theta_t^* - 1}\right) \times \frac{1}{\left(\lambda_{\min}(\hat{G}_t) + \left(\frac{\theta_t^*}{\theta_t^* - 1}\right)\lambda_{\min}(Q^T Q)\right)} \\ &< \frac{1}{\lambda_{\min}(Q^T Q)} = \frac{1}{\underline{q}}. \end{aligned} \tag{44}$$

Based on Equations (28), (29), and (44), we can derive the following:

$$\Pi(\theta_t^*)\|Q^T\|\|\tilde{Q}_t\|\|x_{t-N}\| < \frac{\gamma_Q\gamma_{\tilde{Q}}\rho_x}{\underline{q}}, \tag{45}$$

$$\Pi(\theta_t^*)\|Q^T\|\|\Theta\|\|\omega_{t-N}^{t-1}\| < \frac{\gamma_Q\gamma_{\Theta}(\sqrt{N}\rho_{\omega})}{\underline{q}}, \tag{46}$$

$$\Pi(\theta_t^*)\|Q\|\|v_{t-N}^t\| < \frac{\gamma_Q(\sqrt{N+1}\rho_v)}{\underline{q}}, \tag{47}$$

$$\Pi(\theta_t^*)\|Q\|\|m_{t-N}^t\| < \frac{\gamma_Q\varphi}{\underline{q}}. \tag{48}$$

If Assumptions 1 and 2 are satisfied, we can design a set of scalar parameters

$$\begin{cases} Y_0 = d_1\|x_0 - \bar{x}_0\| + d_2, \\ Y_{t-N} = d_3\|e_{t-N-1,t-1}\| + d_4 + d_5. \end{cases} \tag{49}$$

where

$$\begin{cases} d_1 = \frac{\bar{\sigma}}{\underline{\sigma} + \underline{q}}, \\ d_2 = \frac{(\gamma_Q(\gamma_{\bar{Q}}(\sqrt{N}\rho_\omega) + \gamma_{\Theta}\rho_x + (\sqrt{N+1}\rho_v) + \varphi))}{\underline{q}}, \\ d_3 = \frac{\bar{\sigma}\gamma_a}{\underline{\sigma} + \underline{q}}, \\ d_4 = \frac{\bar{\sigma}(\gamma_{\delta a}\rho_x + \rho_\omega)}{\underline{\sigma} + \underline{q}}, \\ d_5 = \frac{\gamma_Q(\gamma_{\bar{Q}}\rho_x + \gamma_{\Theta}(\sqrt{N}\rho_\omega) + (\sqrt{N+1}\rho_v) + \varphi)}{\underline{q}}. \end{cases} \tag{50}$$

By utilizing Equations (36), (41)–(43), and (45)–(50), we can transform Equation (39) into

$$\begin{aligned} \|\hat{e}_{t-N,t}\| &< \frac{\bar{\sigma}\gamma_a}{\underline{\sigma} + \underline{q}}\|e_{t-N-1,t-1}\| + \frac{\bar{\sigma}\gamma_{\delta a}\rho_x}{\underline{\sigma} + \underline{q}} + \frac{\bar{\sigma}\rho_\omega}{\underline{\sigma} + \underline{q}} + \frac{\gamma_Q\gamma_{\bar{Q}}\rho_x}{\underline{q}} \\ &\quad + \frac{\gamma_Q\gamma_{\Theta}(\sqrt{N}\rho_\omega)}{\underline{q}} + \frac{\gamma_Q(\sqrt{N+1}\rho_v)}{\underline{q}} + \frac{\gamma_Q\varphi}{\underline{q}} \\ &= d_3\|e_{t-N-1,t-1}\| + d_4 + d_5 = Y_{t-N}. \end{aligned} \tag{51}$$

Similarly, at $t \leq N$, $\|e_{0,t}\|$ satisfies

$$\begin{aligned} \|e_{0,t}\| = \|x_0 - \hat{x}_{0,t}\| &< \frac{\bar{\sigma}}{\underline{\sigma} + \underline{q}}\|x_0 - \bar{x}_0\| + \frac{\gamma_Q\gamma_{\bar{Q}}(\sqrt{N}\rho_\omega)}{\underline{q}} \\ &\quad + \frac{\gamma_Q\gamma_{\Theta}\rho_x}{\underline{q}} + \frac{\gamma_Q(\sqrt{N+1}\rho_v)}{\underline{q}} + \frac{\gamma_Q\varphi}{\underline{q}} \\ &= d_1\|x_0 - \bar{x}_0\| + d_2 = Y_0. \end{aligned} \tag{52}$$

In Equation (51), $\|e_{t-N-1,t-1}\|$ needs to be discussed. If $r_{t-1} = 0$, $\|e_{t-N-1,t-1}\| = \|x_{t-N-1} - \tilde{x}_{t-N-1}\| \leq Y$ is obtained from Theorem 1, then $\|x_{t-N} - \hat{x}_{t-N,t}^*\| = \|\hat{e}_{t-N,t}\| \leq d_3Y + d_4 + d_5$ can be obtained. If $r_{t-1} = 1$, $\|e_{t-N-1,t-1}\| = \|x_{t-N-1} - \hat{x}_{t-N-1,t-1}^*\| < Y_{t-N-1}$ is obtained from Equations (38) and (51); then, $\|x_{t-N} - \hat{x}_{t-N,t}^*\| = \|\hat{e}_{t-N,t}\| < d_3Y_{t-N-1} + d_4 + d_5$ can be obtained. \hat{G}_t is selected such that $\|\Xi(\theta_t^*)^{-1}\|\|\hat{G}_t\|\|A\| < 1$ and $\|\Xi(\theta_t^*)^{-1}\|\|\hat{G}_t\| \neq 1$, ($\theta_t^* > 1$), then $d_3 = \bar{\sigma}\gamma_a / (\underline{\sigma} + \underline{q}) \leq 1$ and $d_1 \neq 1$ can be obtained. At the same time, it can be surmised from Ref. [14] and Equation (50) that d_1, d_2, d_4 , and d_5 are bounded parameters. Therefore, we ultimately arrive at the fact that Y_{t-N} is bounded.

Thus, the proof of Theorem 2 is complete. □

Based on the Theorems 1 and 2 and Ref. [25], we can conclude that the state estimation error $e_{t-N,t}$ always satisfies $\|e_{t-N,t}\| \leq \max\{Y_{t-N}, Y, Y_{ss}\}$, regardless of whether the event at the previous time has been triggered. Y_{ss} represents the steady-state value of Y_{t-N} ,

$Y_{ss} = d_2 + d_3/1 - d_1$. Therefore, the stability of the event-triggered state estimation method proposed in this paper has been proven.

5. Simulation Example

A simulation example is introduced in this section to demonstrate that the proposed event state estimation method for uncertain systems with binary-coded communication schemes is feasible.

Consider the uncertain systems described by Equation (1) and let $A = \begin{bmatrix} 1.57 & 0.54 \\ -0.27 & 0.91 \end{bmatrix}$, $C = \begin{bmatrix} 0.9 & 0 \end{bmatrix}$, $\delta A_t = \text{diag}[0.06 \times \sin t \quad 0.09 \times \cos t]$, $\rho_x = 2$, $\rho_\omega = 0.3$, $\rho_v = 0.5$, and $G = \text{diag} \begin{bmatrix} 1.5 & 1.5 \end{bmatrix}$. The state estimation window length N is set to 4, the event-triggered threshold Δ is set to 0.21, and the simulation times are set to 150.

The event-triggered situations of the proposed method with $\Delta = 0.21$ are shown in Figure 4. As we can see from Figure 4, based on the ETM, the MHER and OLER2 in the state estimator operate alternately and efficiently, thus indicating that the efficiency of state estimation has been improved.

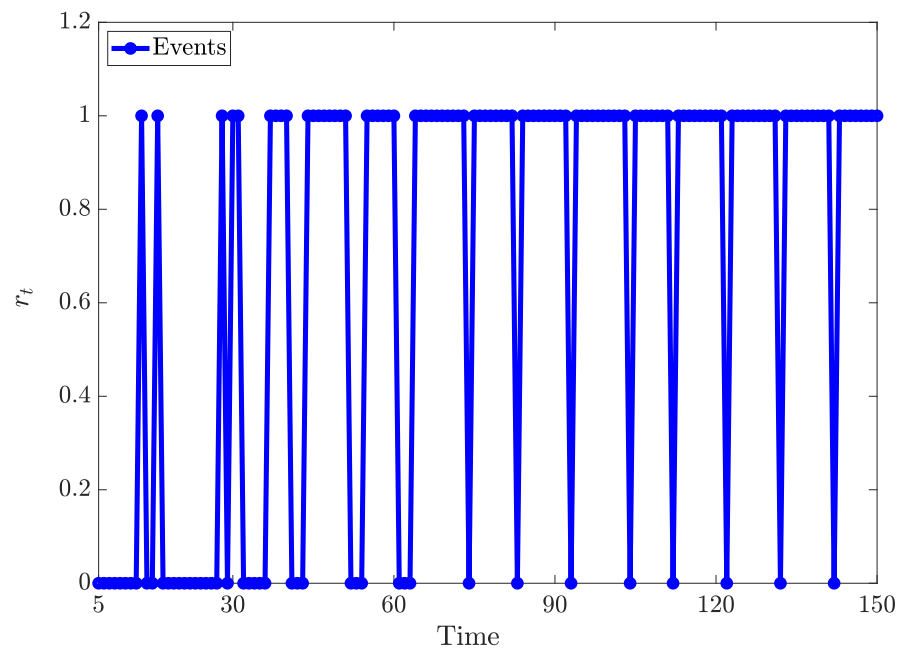


Figure 4. Event-triggered situations at $\Delta = 0.21$.

To demonstrate the good performance of the proposed method (EHME method), this paper compares the EMHE method with the H_∞ Extended Kalman Filter method (HEKF method) proposed in [9] and the robust state estimation method (RBSE method) proposed in [3]. The state estimation results output by the EHME method, the HEKF method, and the RBSE method are shown in Figures 5 and 6, while the state estimation error of the three methods is presented in Figure 7. Figures 5–7 indicate that the EMHE method has a better state-tracking trajectory and a smaller state estimation error compared to the HEKF method and the RBSE method. Therefore, we can conclude that although the proposed method introduces the ETM and the binary encoding transmission scheme, it can still maintain good estimation performance.

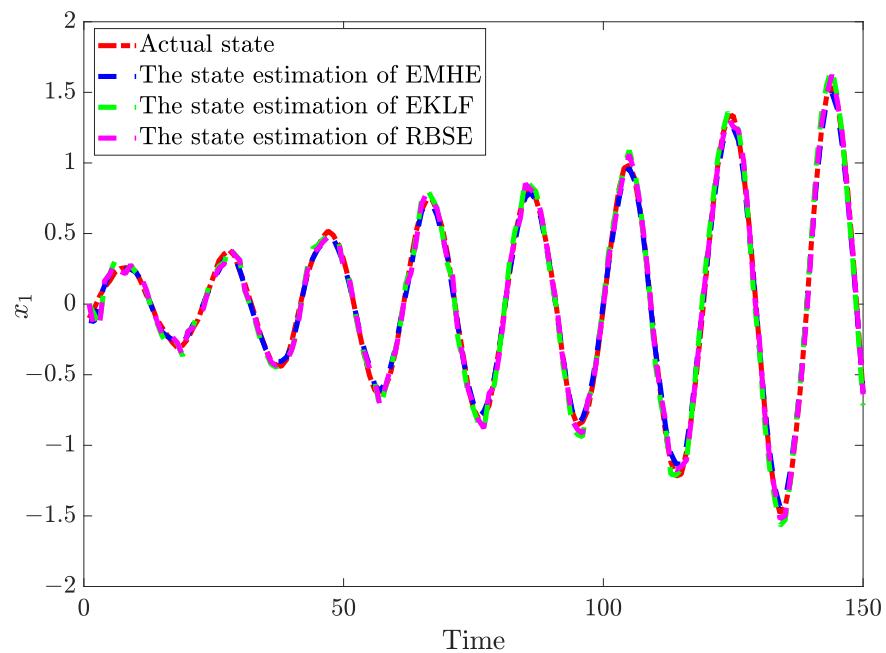


Figure 5. Estimation situations of the state x_1 .

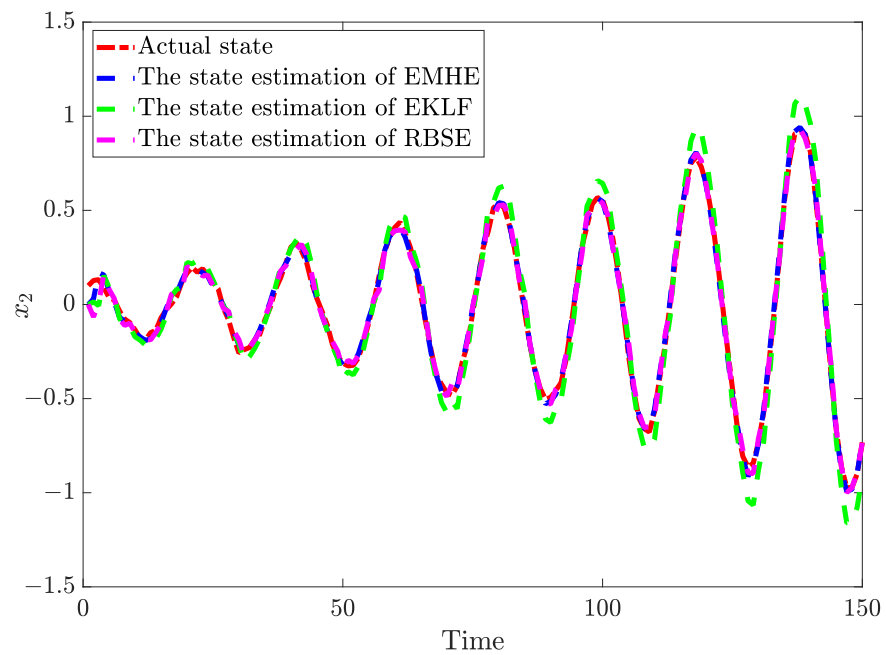


Figure 6. Estimation situations of the state x_2 .

In order to further validate the practical application value of the method proposed in this paper, we calculated the times of the EMHE method, the method without an ETM, the HEKF method, and the RBSE method under the same simulation times and summarized them in Table 1. Since the method without an ETM always uses the MHER with a relatively complex algorithm to estimate the state, its calculation time is the longest. At the same time, since both the HEKF method and the RBSE method are designed on the basis of the Extended Kalman Filter method, the corresponding state estimation also takes a long time. However, the EMHE method reduces the use of the MHER and significantly shortens the computational time by introducing the an ETM. When the simulation times are set to 150, compared with the method without an ETM, the HEKF method, and the RBSE method, the EMHE method reduced the required time by 63.05% , 45.36%, and 51.69%, respectively.

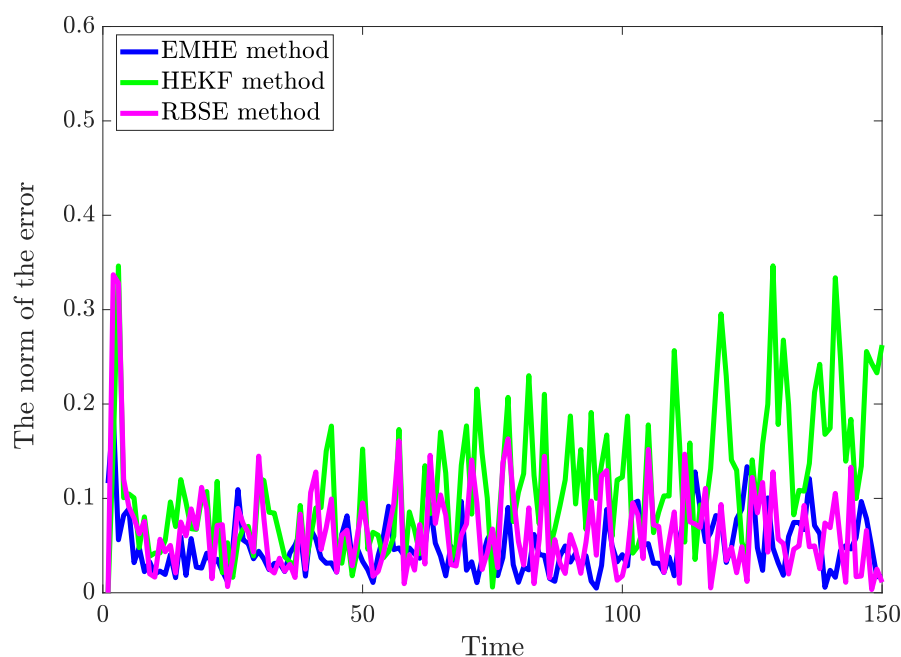


Figure 7. State estimation error of the three methods.

Table 1. Calculation time(s) of the four methods at different simulation times j .

j	50	100	150
EMHE method	0.3572	1.0386	2.1563
The method without an ETM	1.4847	3.3549	5.8354
HEKF method	1.2131	2.5514	3.9462
RBSE method	1.3524	2.8647	4.4635

According to the above analysis, we can conclude that the method proposed in this paper saves network communication resources, reduces the computational burden of the estimator, ensures the stability of state estimation, and improves the state estimation performance of uncertain systems.

6. Conclusions

This paper proposes an event-triggered state estimation method for uncertain systems with a binary encoding transmission scheme. A binary encoding transmission scheme is introduced to ensure the remote and efficient transmission of information between a state estimator and a system. An ETM is incorporated to save network bandwidth and improve computational efficiency. an MHER is designed for optimal state estimation using the robust least squares optimization approach when an event is triggered, and the simpler OLER is used for state estimation when an event is not triggered. Stability analysis proved that the state estimation error is bounded. Finally, the proposed method’s improvement in addressing estimation problems was validated through a simulation example.

Future work will investigate the design of an adaptive event-triggered mechanism for uncertain linear systems and distributed uncertain systems to further optimize state estimation methods.

Author Contributions: Conceptualization, Z.L. and B.X.; methodology, Z.L. and B.X.; software, Z.L.; data curation, Z.L.; writing—original draft preparation, Z.L. and Y.C.; writing—review and editing, Z.L. and Y.C.; funding acquisition, Z.L. All authors have read and agreed to the published version of the manuscript.

Funding: This work was supported in part by the National Natural Science Foundation of China under Grant 61603205, in part by the China Postdoctoral Science Foundation under Grant 2017M612205.

Data Availability Statement: Not applicable.

Conflicts of Interest: The authors declare no conflict of interest.

References

1. Xue, B.Q.; Li, S.Q.; Zhu, Q.M. Moving Horizon State Estimation for Networked Control Systems with Multiple Packet Dropouts. *IEEE Trans. Autom. Control* **2012**, *57*, 2360–2366. [[CrossRef](#)]
2. Heo, S.; Park, C.G. Consistent EKF-based visual-inertial odometry on matrix Lie group. *IEEE Sens. J.* **2018**, *18*, 3780–3788. [[CrossRef](#)]
3. Wang, J.; Mao, Y.; Li, Z.Q.; Gao, J.W.; Liu, H.B. Robust state estimation for uncertain linear discrete systems with d-step state delay. *IET Control Theory Appl.* **2021**, *15*, 1708–1723. [[CrossRef](#)]
4. Rengaswamy, R.; Narasimhan, S.; Kuppuraj, V. Receding-Horizon Nonlinear Kalman (RNK) Filter for State Estimation. *IEEE Trans. Autom. Control* **2013**, *58*, 2054–2059. [[CrossRef](#)]
5. Huang, Z.H.; Guo, Y.R.; Peng, H.; Xu, Y. Distributed Moving Horizon Estimation Over Wireless Sensor Networks: A Matrix-Weighted Consensus Approach. *IEEE Trans. Circuits Syst. II Express Briefs* **2023**, *70*, 1665–1669. [[CrossRef](#)]
6. Rao, C.; Rawlings, J.; Lee, J. Constrained Linear State Estimation—A Moving Horizon Approach. *Automatica* **2001**, *37*, 1619–1628. [[CrossRef](#)]
7. Sui, D.; Johansen, A.; Feng, L. Linear Moving Horizon Estimation with Pre-Estimating Observer. *IEEE Trans. Autom. Control* **2010**, *55*, 2363–2368. [[CrossRef](#)]
8. Battistelli, G. Distributed Moving-Horizon Estimation with Arrival-Cost Consensus. *IEEE Trans. Autom. Control* **2019**, *64*, 3316–3323. [[CrossRef](#)]
9. Zhao, J. Dynamic State Estimation With Model Uncertainties Using H_∞ Extended Kalman Filter. *IEEE Trans. Power Syst.* **2018**, *33*, 1099–1100. [[CrossRef](#)]
10. Qian, C.J. Semi-global stabilization of a class of uncertain nonlinear systems by linear output feedback. *IEEE Trans. Circuits Syst. II Express Briefs* **2005**, *52*, 218–222. [[CrossRef](#)]
11. Guo, G.; Wang, B.F. Robust kalman filtering for uncertain discrete-time systems with multiple packet dropouts. *Acta Autom. Sin.* **2010**, *36*, 767–772. [[CrossRef](#)]
12. Sayed, A.; Nascimento, V.; Cipparrone, F. A Regularized Robust Design Criterion for Uncertain Data. *SIAM J. Math. Anal.* **2002**, *23*, 1120–1142. [[CrossRef](#)]
13. Liu, S.; Zhao, G.R.; Zeng, B.; Gao, C. Moving Horizon Estimation for Uncertain Systems With Packet Dropouts and Quantization. *J. Syst. Eng. Electron.* **2020**, *42*, 912–918.
14. Alessandri, A.; Baglietto, M.; Battistelli, G. Robust Receding Horizon Estimation for Uncertain Discrete time Linear Systems. *IEEE Control Syst. Lett.* **2003**, *54*, 627–643. [[CrossRef](#)]
15. Wang, S.D.; Xue, B.Q. Distributed Moving Horizon Fusion Estimation for Nonlinear Constrained Uncertain Systems. *Mathematics* **2023**, *11*, 1507. [[CrossRef](#)]
16. Zhao, K.H. Stability of a Nonlinear Langevin System of ML-Type Fractional Derivative Affected by Time-Varying Delays and Differential Feedback Control. *Fractal Fract.* **2022**, *6*, 725. [[CrossRef](#)]
17. Xu, Y.; Zhou, J.Y.; Rao, H.X.; Lu, R.Q.; Xie, L.H. Reset Moving Horizon Estimation for Quantized Discrete Time Systems. *IEEE Trans. Autom. Control* **2021**, *66*, 4199–4205. [[CrossRef](#)]
18. Alessandri, A.; Baglietto, M.; Battistelli, G. Receding-horizon Estimation for Discrete Time Linear Systems. *IEEE Trans. Autom. Control* **2003**, *48*, 473–478. [[CrossRef](#)]
19. Liu, A.; Yu, L.; Zhang, W.A.; Chen, M. Moving Horizon Estimation for Networked Systems with Quantized Measurements and Packet Dropouts. *IEEE Trans. Circuits Syst. II Express Briefs* **2012**, *60*, 1823–1834. [[CrossRef](#)]
20. Xue, B.Q.; Li, N.; Li, S.Y.; Zhu, Q.M. Moving Horizon Scheduling for Networked Control Systems with Communication Constraints. *IEEE Trans. Ind. Electron.* **2013**, *60*, 3318–3327. [[CrossRef](#)]
21. Zhou, H.D.; Sui, S.; Tong, S.C. Finite-Time Adaptive Fuzzy Prescribed Performance Formation Control for High-Order Nonlinear Multiagent Systems Based on Event-Triggered Mechanism. *IEEE Trans. Fuzzy Syst.* **2023**, *31*, 1229–1239. [[CrossRef](#)]
22. Wang, Y. An Event-Triggered Scheme for State Estimation of Preceding Vehicles under Connected Vehicle Environment. *IEEE Trans. Veh. Technol.* **2023**, *8*, 583–593.
23. Zhong, M.; Du, X.; Song, Y.; Xue, T.; Ding, S.X. Event-Triggered Parity Space Approach to Fault Detection for Linear Discrete-Time System. *IEEE Trans. Syst. Man Cybern. Syst.* **2022**, *52*, 4813–4822. [[CrossRef](#)]
24. Huang, J.R.; Shi, D.W.; Chen, T.W. Event-triggered State Estimation with an Energy Harvesting Sensor. *IEEE Trans. Autom. Control* **2017**, *62*, 4768–4775. [[CrossRef](#)]
25. Yin, X.Y.; Liu, J.F. Event-triggered State Estimation of Linear Systems Using Moving Horizon Estimation. *IEEE Trans. Control Syst. Technol.* **2021**, *29*, 901–909. [[CrossRef](#)]
26. Yin, X.Y.; Huang, B. Event-triggered Distributed Moving Horizon State Estimation of Linear Systems. *IEEE Trans. Syst. Man Cybern. Syst.* **2022**, *52*, 6439–6451. [[CrossRef](#)]
27. Alessandri, A.; Awawdeh, M. Moving-horizon estimation with guaranteed robustness for discrete-time linear systems and measurements subject to outliers. *Automatica* **2016**, *67*, 85–93. [[CrossRef](#)]

28. He, D.; Xu, C.; Zhu, J.; Du, H. Moving horizon H_∞ estimation of constrained multisensor systems with uncertainties and fading channels. *IEEE Trans. Instrum. Meas.* **2021**, *70*, 1–12. [[CrossRef](#)]
29. Schiller, J.D.; Müller, M.A. Suboptimal Nonlinear Moving Horizon Estimation. *IEEE Trans. Autom. Control* **2023**, *68*, 2199–2214. [[CrossRef](#)]
30. Zou, L.; Wang, Z.D.; Hu, J.; Han, Q.L. Moving Horizon Estimation With Unknown Inputs under Dynamic Quantization Effects. *IEEE Trans. Autom. Control* **2020**, *65*, 5368–5375. [[CrossRef](#)]
31. Liu, Q.Y.; Wang, Z.D. Moving-horizon Estimation for Linear Dynamic Networks with Binary Encoding Schemes. *IEEE Trans. Autom. Control* **2021**, *66*, 1763–1770. [[CrossRef](#)]
32. Alessandri, A.; Baglietto, M.; Battistelli, G. Moving-horizon state estimation for nonlinear discrete-time systems: New stability results and approximation schemes. *Automatica* **2008**, *7*, 1753–1765. [[CrossRef](#)]
33. Farina, M.; Ferrari-Trecate, G.; Scattolini, R. Distributed Moving Horizon Estimation for Linear Constrained Systems. *IEEE Trans. Autom. Control* **2010**, *55*, 2462–2475. [[CrossRef](#)]
34. Gharbi, M.; Gharesifard, B.; Ebenbauer, C. Anytime Proximity Moving Horizon Estimation: Stability and Regret. *IEEE Trans. Autom. Control* **2023**, *68*, 3393–3408. [[CrossRef](#)]
35. Zhao, K.H. Solvability and GUH-stability of a nonlinear CF-fractional coupled Laplacian equations. *AIMS Math.* **2023**, *8*, 13351–13367. [[CrossRef](#)]
36. Zhao, K.H. Existence and Stability of a Nonlinear Distributed Delayed Periodic AG-Ecosystem with Competition on Time Scales. *Axioms* **2023**, *12*, 315. [[CrossRef](#)]
37. Ji, L.; Rawlings, B.J.; Hu, W.; Wynn, A.; Diehl, M. Robust Stability of Moving Horizon Estimation Under Bounded Disturbances. *IEEE Trans. Autom. Control* **2016**, *61*, 3509–3514. [[CrossRef](#)]

Disclaimer/Publisher’s Note: The statements, opinions and data contained in all publications are solely those of the individual author(s) and contributor(s) and not of MDPI and/or the editor(s). MDPI and/or the editor(s) disclaim responsibility for any injury to people or property resulting from any ideas, methods, instructions or products referred to in the content.